CREST LEVEL OPTIMIZATION OF THE MULTI LEVEL OVERTOPPING BASED WAVE ENERGY CONVERTER SEAWAVE SLOT-CONE GENERATOR

J. P. Kofoed[1] and E. Osaland[2]

[1]Department of Civil Engineering, Aalborg University, Denmark
i5jpk@civil.aau.dk, +45 9635 8474
[2]WAVEenergy AS, Aalgaard, Norway
espen.osaland@waveenergy.no, +47 5161 0931

ABSTRACT

The paper describes the optimization of the crest levels and geometrical layout of the SSG structure, focusing on maximizing the obtained potential energy in the overtopping water.

During wave tank testing at AAU average overtopping rates into the individual reservoirs have been measured. The initial tests led to an expression describing the derivative of the overtopping rate with respect to the vertical distance. Based on this, numerical optimizations of the crest levels, for a number of combinations of wave conditions, have been performed. The hereby found optimal crest levels have been tested in the wave tank and further optimizations of the geometry have been carried out.

INTRODUCTION

The Seawave Slot-cone Generator (SSG) is a multi level wave energy converter (WEC) based on the wave overtopping principle, being developed by the Norwegian company WAVEenergy AS (WE). The device is utilizing a total of three reservoirs placed on top of each other, in which the potential energy of the incoming waves is stored. The water captured in the reservoirs then run through the multi-stage turbine (MST). Using multiple reservoirs results in a higher overall efficiency, compared to a single reservoir structure. The device is illustrated in figure 1.

The SSG is built as a robust concrete structure with the turbine shaft and the gates controlling the water flow as virtually the only moving part of the mechanical system.

The SSG concept makes use of the innovative patent pending multi-stage turbine also developed by WE. The MST has the advantage to utilize different heights of water head on a common turbine wheel. The multi-stage technology minimize the number of start/stop sequences on the turbine, even if only one reservoir is supplying water to the turbine, resulting in a high degree of utilization.

SINTEF Energiforskning AS (SEfAS) and the Norwegian University of Science and Technology (NTNU) has performed a 3D CFD analysis of the guide vane and the runner, based on the Euler turbine equation. This shows an estimated efficiency on the individual stages of the MST of ~90 % with a

Figure 1. Illustration of the SSG structure.

relative flat efficiency curve. The performance of the MST under simultanous varying conditions on the different stages is currently being investigated.

The purpose of the work described in the paper has been to optimize the crest levels and geometrical layout of the SSG structure in a combination of irregular wave conditions, focusing on maximizing the obtained potential energy in the overtopping water.

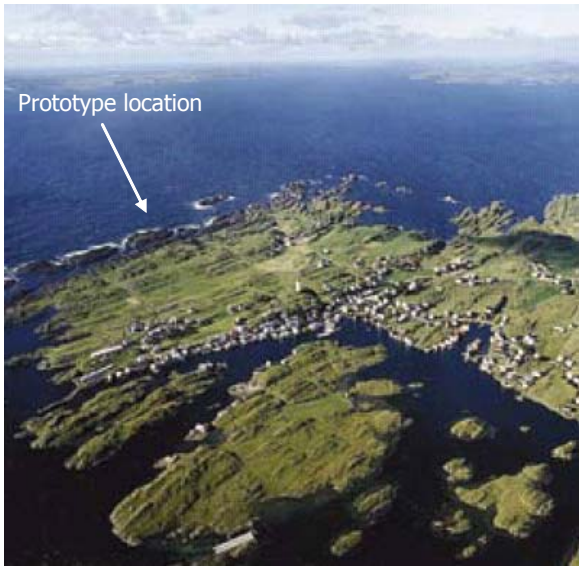

Figure 2. Planned prototype location.

The work is done as a part of the preparation of the pilot project where a full-scale technical prototype of the SSG breakwater structure which is planned for installation on the west coast of the island of Kvitsøy in an 19 kW/m wave climate, marked in figure 2. The pilot project is part funded by European Commision FP6-2004-Energy3.

Wave data recordings have been carried out from 3. November 2004 to 30. April 2005 in order to determine the wave climate on the test site and to give input to design parameters for the SSG and the turbine. The pilot structure is planned to be a 10 m wide module, with approx. 200 kW installed capacity.

Model tests have been performed in a wave tank at Aalborg University (AAU). Here average overtopping rates into the individual overtopping reservoirs have been measured. The initial tests provided data allowing for the formulation of an expression describing the derivative of the overtopping rates with respect to the vertical distance. Based on this expression numerical optimizations of the crest levels for a number of combinations of wave conditions have been performed. The hereby found optimal crest levels have then been tested in the wave tank and further optimizations of the geometry will also be carried out.

MODEL TESTS

In two rounds model tests have been performed in the deep water 3-D wave basin at the Hydraulics and Coastal Engineering Laboratory, AAU. The tests have been performed using a length scale of 1:15 and 1:25, compared to the planned prototype. During these tests average overtopping rates into the individual reservoirs, as well as the waves have been measured.

Setup

The model test setup primarily consists of 3 components, see figure 3:

1. Leading walls (with a distance equal to the width of the test section, 0.5 m, model scale) was installed in front of the test section, in order to have well defined 2-D incoming waves. The incoming waves were measured by three wave gauges placed be between the leadings walls (in the hereby established flume) in front of the test section. Furthermore, a single wave gauge was deployed outside the flume, allowing for comparisons.
2. The test section. The tested geometries are described in the following section. The three reservoirs were connected by large dimension hoses to reservoir tanks outside the wave tank.
3. Reservoir tanks. Each of the three reservoirs in the test section has a reservoir tank which is used to measure the amount of overtopping in the individual reservoir. In each reservoir tank a level gauge and a pump was placed. The level gauge and the pump were connected to a PC programmed to empty the reservoir tanks and thereby recording the amount of water overtopping into the individual reservoirs.

Figure 3. Model test setup.

Prior to the testing the wave gauge, level gauges, volume of reservoir tanks and pump capacities have been calibrated.

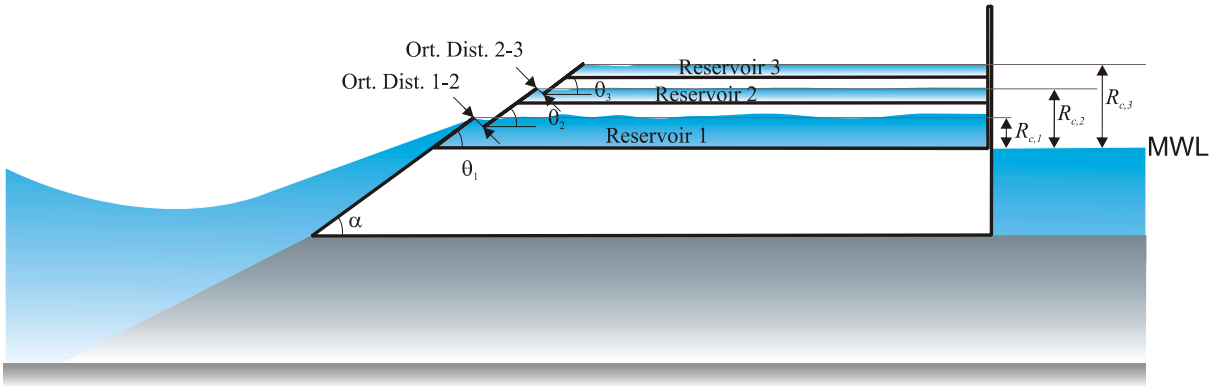

Figure 4. Illustration of parameters describing the tested geometries.

Tested geometries

A total of 17 different geometries have been tested, 10 in the first round and 7 in the second. The principal layout of the tested geometries is illustrated in figure 4. The first 10 geometries have been tested using a length scale of 1:15 and a water depth of 6.0 m, corresponding to the local water depth at the deployment site (tests A1-E2). The structure was in these tests placed directly on a horizontal seabed. All 10 geometries had crest levels of 2.25, 3.30 and 4.65 m for reservoirs 1, 2 and 3, respectively, except for the last two tests (E, E2) where the crest level of the lowest reservoir was changed to 1.5 m. The angle α of the front slope was changed from 19° to 35° through the first round.

After the first round of tests it was found that placing the structure directly on a horisontal seabed did not represent the reality well, as the rocky shoreline at the site was seen from charts to be rather steep. This was taken into account in the second round of testing where the water depth was increased to 25 m, and a 1:2 slope leading up to the structure was used (tests F1-F7). In order to accommodate this in the wave basin, and to facilitate handling of the large quantities of overtopping water, the length scale was set at 1:25 in the second round of testing. During these tests crest levels of 1.5, 3.0 and 5.0 m for reservoirs 1, 2 and 3, respectively, was used, except for the first geometry (F1), where the crest levels of reservoir 2 and 3 were 2.5 and 4.0 m, respectively.

Wave conditions

Based on wave data from DNMI and Torsethaugen (1990) the offshore wave climate near the deployment site was esimated to as given in table 1. These wave conditions were used as target in the generation of the irregular waves in the model tests.

In the first round of testing wave conditions 1-5 were used. However, due to the relatively low water level, quit severe wave breaking occurred in wave conditions 3-5. In the second round of testing wave conditions 1-7 were applied and here only limited wave breaking occurred and only in the largest wave conditions.

The available wave power averaged with probability over these 6 wave conditions is P_{wave} = 31.7 kW/m. These wave conditions covers 86.5 % of the time. Of the remaining 13.5 %, 12.6 % corresponds to wave conditions with H_s < 1 m and 0.6 % corresponds to wave conditions with H_s > 7 m.

Table 1
Wave conditions as applied in model tests.

Wave condition	1-2	2-3	3-4	4-5	5-6	6-7
Hs [m]	1.5	2.5	3.5	4.5	5.5	6.5
Tp [s]	6.12	7.90	9.34	10.60	11.71	12.73
Te [s]	5.32	6.87	8.13	9.21	10.19	11.07
Pwave [kW/m]	5.9	21.0	48.8	91.4	151.0	229.2
Probability [%]	30.3	26.5	16.4	8.3	3.5	1.5

RESULTS AND DISCUSSION

First round

Based on the results of the first round of model tests it was found, for the wave conditions given in table 1, that the crest levels used here was probably not the optimal ones. This was indicated by the fact that significantly larger efficiencies was optained for geometry E, which has a lower crest level for the lowest reservoir, than in the other geometries.

In order to enable optimization of crest levels for the three reservoirs, data from geometry D and E (which are identical in setup, except for a change in crest level) was used to determine the empirical coefficients A, B and C in the expression by Kofoed (2002)

$$Q' = \frac{dq/dz}{\sqrt{gH_s}} = Ae^{B\frac{z}{H_s}+C\frac{R_{c,1}}{H_s}} \qquad (1)$$

where Q' is the dimensionless derivative of the overtopping rate with respect to the vertical distance z.

By non-linear regression analysis the coefficients A, B and C has been found to be 0.197, -1.753 and -

0.408, respectively. For comparison the coefficients A, B and C was found by Kofoed (2002) to be 0.37, -4.5 and 3.5, respectively, for model tests with reservoirs without fronts mounted.

Based on the equation above overtopping rates for individual reservoirs can be estimated using

$$\begin{aligned} q_n(z_1,z_2) &= \int_{z_1}^{z_2} {}^{dq}\!/_{dz}\, dz \\ &= \int_{z_1}^{z_2} \sqrt{gH_s}\, A e^{B\frac{z}{H_s}} e^{C\frac{R_{c,1}}{H_s}} dz \\ &= \sqrt{gH_s^3}\,\frac{A}{B} e^{C\frac{R_{c,1}}{H_s}} \left(e^{B\frac{z_2}{H_s}} - e^{B\frac{z_1}{H_s}} \right) \end{aligned} \quad (2)$$

where z_1 and z_2 denote the lower and upper vertical boundary of the reservoir, respectively. Generally, $z_1 = R_{c,n}$ and $z_2 = R_{c,n+1}$ is used, n being the reservoir number. However, for the top reservoir z_2 is in principle infinite, but has here been set at 10 m (full scale).

The optimal crest levels of the three reservoirs was then found by using eq. (2) in a numerical optimization. Here, the overall hydraulic efficiency, defined as the ratio $\Sigma P_{total} \cdot Prob$ / $\Sigma P_{wave} \cdot Prob$ (i.e. the ratio between the potential power in the overtopping water at the time the water overtops the crests, and the available power in the incoming waves) for the considered wave conditions was used as optimization parameter.

This optimization gave 1.5, 3.0 and 5.0 m as optimal crest levels for reservoir 1, 2 and 3, resulting in an overall hydraulic efficiency of 44.0 % for the considered wave conditions given in table 1.

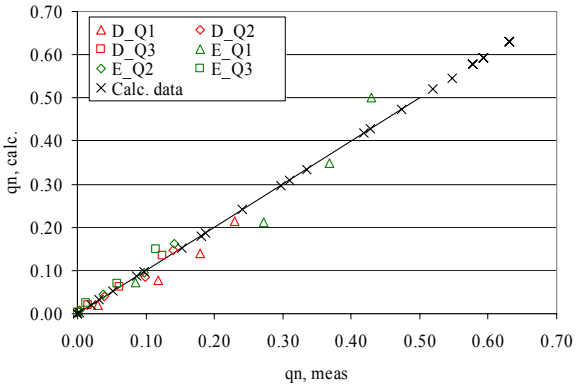

Figure 5. Comparison of calculated and measured data. The black x's represents data points found in the optimization of the crest levels.

Second round

Based on the above the second round of model tests were planned. All but one of the geometries used in these tests, were with crest levels as given above. The purpose of the second round of tests were to check the result of the numerical optimization and to further optimize the geometry by testing changes in the geometries other than the crest levels. The results of the second round of tests are given in table 2. Here the results of the second round of model tests are presented in terms of full scale overtopping rates (q_n, n indicating the reservoir number) and hydraulic power in each of the three reservoirs (P_n, n, found as the overtopping rate times the crest level of the reservoir times the acceleration of gravity), and the total overtopping rate (q_{total}, the sum of q_n) and total hydraulic power (P_{total}, the sum of P_n) and efficiency (defined as the ratio between P_{total} and P_{wave}) for the individual tests.

From here it is seen that an overall hydraulic efficiency over wave conditions 1-7 of 51.8 % has been achieved for geometry F7, which is considered the optimal for the given wave conditions. This is significantly higher than the result of the numerical optimization based on the results of the first round of model tests.

The reasons for this is considered primarely to be the change in water depth from first to second round, together with the fact that the geometrical changes, other than the crest levels, tested in the second round have optimized the structure significantly. Furthermore, eq. (2), used in the numerical optimization, was based on a relatively small data set, i.e. some uncertainty must be expected.

The increase in performance is also illustrated in figure 6 where the results for geometry F7 are compared to eq. (2).

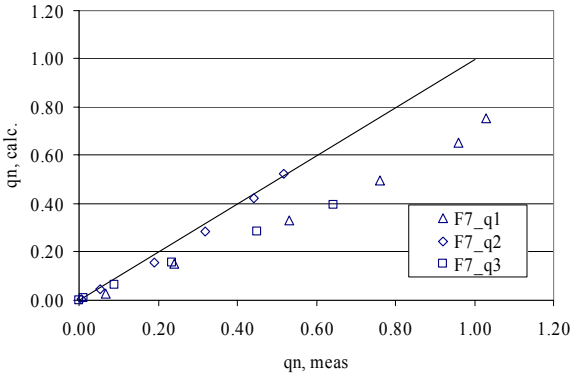

Figure 6. Comparison of eq. (2) (straight line) and measured data for geometry F7.

Table 2.
Results of the second round of model tests, given in terms of full scale overtopping rates and hydraulic power in the three reservoirs, and the total power and efficiency for the individual tests. For each geometry the overall efficiency is also given (for F1-6 the efficiency (eff.) is based on wave conditions 1-2, 3-4 and 5-6, for F7 the efficiency based on all 6 wave conditions (eff. all) is also given).

Geometry	Wave cond.	q1 [m^3/s/m]	q2 [m^3/s/m]	q3 [m^3/s/m]	qtotal [m^3/s/m]	P1 [kW/m]	P2 [kW/m]	P3 [kW/m]	Ptotal [kW/m]	eff. [-]
F1	1-2	0.047	0.014	0.002	0.062	0.70	0.35	0.08	1.13	0.289
eff	2-3	0.190	0.106	0.050	0.345	2.86	2.66	2.00	7.52	0.540
0.469	5-6	0.482	0.442	0.542	1.466	7.28	11.12	21.82	40.22	0.454
F2	1-2	0.060	0.007	0.000	0.067	0.91	0.20	0.02	1.13	0.290
eff	3-4	0.488	0.207	0.103	0.798	7.37	6.25	5.16	18.78	0.569
0.526	5-6	0.814	0.441	0.441	1.695	12.29	13.32	22.17	47.78	0.540
F3	1-2	0.056	0.007	0.001	0.063	0.84	0.22	0.03	1.08	0.277
eff	3-4	0.461	0.212	0.108	0.780	6.96	6.39	5.43	18.77	0.569
0.522	5-6	0.738	0.450	0.448	1.636	11.14	13.59	22.56	47.29	0.534
F4	1-2	0.058	0.006	0.000	0.065	0.88	0.18	0.01	1.07	0.275
eff	3-4	0.480	0.196	0.079	0.755	7.25	5.91	4.00	17.16	0.520
0.504	5-6	0.880	0.470	0.447	1.797	13.29	14.18	22.49	49.96	0.564
F5	1-2	0.059	0.005	0.000	0.064	0.88	0.16	0.02	1.06	0.272
eff	3-4	0.498	0.199	0.073	0.770	7.52	6.01	3.67	17.19	0.521
0.502	5-6	0.940	0.478	0.410	1.828	14.19	14.43	20.64	49.26	0.557
F6	1-2	0.066	0.004	0.000	0.070	1.00	0.12	0.01	1.12	0.288
eff	3-4	0.543	0.198	0.080	0.821	8.20	5.99	4.01	18.20	0.551
0.511	5-6	0.924	0.444	0.380	1.748	13.94	13.41	19.15	46.50	0.525
F7	1-2	0.067	0.004	0.000	0.071	1.01	0.13	0.01	1.15	0.295
eff	2-3	0.239	0.054	0.010	0.303	3.61	1.63	0.51	5.75	0.413
0.528	3-4	0.532	0.191	0.089	0.812	8.03	5.78	4.49	18.29	0.554
	4-5	0.761	0.318	0.235	1.314	11.49	9.60	11.84	32.93	0.571
eff,all	5-6	0.961	0.443	0.451	1.854	14.50	13.38	22.68	50.56	0.571
0.518	6-7	1.030	0.517	0.644	2.191	15.55	15.62	32.40	63.56	0.545

It is seen that the incerase in performance is due to considerably larger measured overtopping rates for reservoir 1 and 3 compared to the expression based on the previous model test. For reservoir 2 the expression seems to predict the overtopping rates very well.

Wave direction and structure orientation

After the second round of model testing had been performed, a study of the wave conditions at the prototype location by Kofoed & Guinot (2005) was concluded. This study includes information about wave directions and change in wave conditions due to the bathymetry in the area, and thus gives the near shore wave conditions. These are given in table 3.

The available wave power averaged with probability over these 6 wave conditions for the near shore prototype location is P_{wave} = 18.1 kW/m.

By inter- and extrapolation of the model tests results for geometry F7, overtopping rates and hydraulic power production, have been estimated for all the relevant wave conditions and directions. The estimated overtopping rates are given in figure 7 together with original model test data.

The extrapolation of the overtopping data to wave conditions significantly higher than the ones tested, is obviously relatively uncertain. However, as it is seen from figure 7 the overtopping rates into reservoir 1 and 2 has been estimated to be close to maximum in the largest of the tested wave conditions.

Table 3.
Near shore wave conditions in terms of significant wave height, peak period, direction and probability of occurrence, Kofoed & Guinot (2005). The available wave power in the individual wave conditions is also given, as well as the overall average.

Wave condition	**1-2**	**2-3**	**3-4**	**4-5**	**5-6**	**6-7**	**Sum**
Tp [s]	**6.1**	**7.9**	**9.3**	**10.6**	**11.7**	**12.7**	
Hs [m] **NW-315**	1.2	1.7	2.2	2.6	3.2	4.4	
Dir [deg.]	315	313	310	308	305	303	
Prob	9.9%	8.7%	5.4%	2.7%	1.1%	0.5%	**28.4%**
Pwave [kW/m]	3.8	10.0	18.7	29.8	52.7	106.1	
Pwave*Prob	0.382	0.873	1.007	0.811	0.604	0.522	**4.2**
Hs [m] **W-270**	1.3	2.3	3.4	4.6	5.9	7.4	
Dir [deg.]	270	273	275	278	280	283	
Prob	4.8%	4.2%	2.6%	1.3%	0.6%	0.2%	**13.7%**
Pwave [kW/m]	4.4	17.1	44.9	97.3	176.5	298.1	
Pwave*Prob	0.213	0.716	1.164	1.277	0.976	0.707	**5.1**
Hs [m] **SW-225**	0.8	1.7	2.9	4.1	5.3	6.5	
Dir [deg.]	225	230	235	240	245	250	
Prob	7.5%	6.5%	4.0%	2.0%	0.9%	0.4%	**21.3%**
Pwave [kW/m]	1.6	9.8	34.4	77.7	139.4	229.4	
Pwave*Prob	0.119	0.638	1.390	1.590	1.204	0.849	**5.8**
Hs [m] **S-180**	0.6	1.0	1.2	3.2	4.2	5.5	
Dir [deg.]	225	228	230	233	235	238	
Prob	8.1%	7.1%	4.4%	2.2%	0.9%	0.4%	**23.1%**
Pwave [kW/m]	0.8	3.2	5.3	47.6	89.7	161.8	
Pwave*Prob	0.065	0.227	0.233	1.056	0.839	0.649	**3.1**
Sum							
Prob	**30.3%**	**26.5%**	**16.4%**	**8.3%**	**3.5%**	**1.5%**	**86.5%**
Pwave*Prob	**0.8**	**2.5**	**3.8**	**4.7**	**3.6**	**2.7**	**18.1**

The reasoning behind this estimate is that the size of the gaps between reservoir 1-2 and 2-3 (controlled by the orthogonal distance between the reservoir fronts) are setting an upper limit to the overtopping rates into reservoir 1 and 2. The tendency that the overtopping rates are reaching a maximum value is also seen in the data, especially for reservoir 1. For reservoir 3 there is no such upper limit for the overtopping rate, as there is no structure above it. In the extrapolation it is therefore assumed that the

increasing tendency for the overtopping rate is continued.

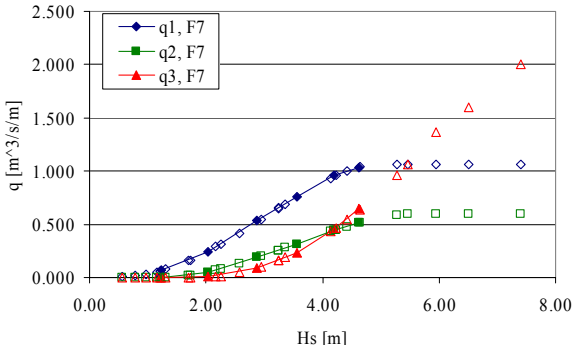

Figure 7. Model test results for geometry F7 (full markers), together with inter- and extrapolated data corresponding to near shore prototype location wave conditions (open markers).

Based on these estimated data the overall average hydraulic efficiency at the prototype location is 50.9 % for near shore wave conditions corresponding to the offshore wave conditions 1-7 as given in table 3. This corresponds to an overall average hydraulic power production of 9.2 kW/m.

However, in these data the effect of orientation of the structure has not been taken into account, ie. it is assumed the structure is facing directly towards the incoming waves, regardless of wave direction.

A factor accounting for oblique wave attack on single reservoir geometries is suggested by Van der Meer & Janssen (1995)

$$\gamma_\beta = 1 - 0.0033\beta \qquad (3)$$

where β is the difference between wave direction and orientation of the structure, measured in degrees, for overtopping rates. γ_β is used by dividing the relative crest freeboard R with it. Eq. (3) is not directly applicable to multi level geometries, but in lack of alternatives a correction factor λ_β is defined as

$$\lambda_\beta = \frac{0.2e^{-2.6\frac{R_{c,n}}{H_s}\frac{1}{\gamma_\beta}}}{0.2e^{-2.6\frac{R_{c,n}}{H_s}}} = e^{-2.6\frac{R_{c,n}}{H_s}\left(\frac{1}{\gamma_\beta}-1\right)} \qquad (4)$$

This correction factor has been calculated based on the wave data in table 4 and multiplied onto the estimated overtopping rates (given in figure 7).

By this procedure it is found that the overall average hydraulic efficiency at the prototype location for a structure facing due west (270°) is 41.4 % for near shore wave conditions corresponding to the offshore wave conditions 1–7, as given in table 4. This corresponds to an overall average hydraulic power production of 7.5 kW/m.

The optimal orientation of the structure has been found by maximizing the overall hydraulic efficiency by changing the orientation. The optimal orientation is found to be in the 250° - 270° range.

The correction factor given in eq. (3) has been derived from model tests with 2-D waves and shore protection structures (breakwaters and dikes), and not a multi level structure with a relatively small width as the SSG structure. Thus, there is a considerable uncertainty in using it for the current purpose and 3-D tests with more detailed modelling of foreshore and structure is needed in order to include refraction/diffraction effects around the structure.

Comparison to existing overtopping expression

As a check of the measured overtopping rates the total overtopping rates in all three reservoirs have been summed for the individual tests and made non-dimensional as suggested by Van der Meer & Janssen (1995)

$$Q = 0.2e^{-2.6R} \qquad (5)$$

where

$Q = \dfrac{q}{\lambda_s\sqrt{gH_s}}$ is the non-dimensional overtopping rate.

$\lambda_s = \begin{cases} 0.4\sin\left(\frac{2\pi}{3}R\right)+0.6 & for \quad R < 0.75 \\ 1 & for \quad R \geq 0.75 \end{cases}$ accounts for low relative crest freeboards, as suggested by Kofoed (2002).

R is the relative crest freeboard, R_c/H_s. Here set at $R_{c,l}/H_s$.

The results hereof are generally in line with eq. (5), as illustrated in figure 8, and thus agrees with well established data from the literature.

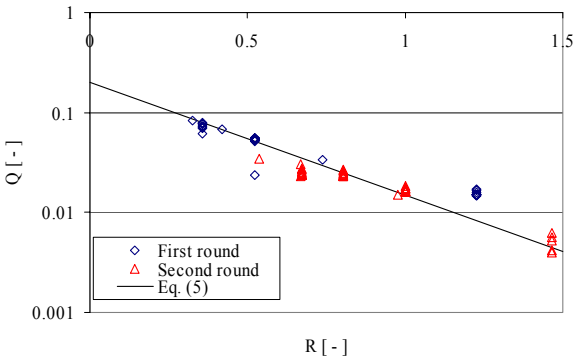

Figure 8. Non-dimensional overtopping rates as a function of the non-dimensional crest freeboard

based on the crest level of the lowest reservoir. The straight line represents eq. (5).

CONCLUSION

The optimization of the crest levels and geometrical layout of the SSG structure has been described. Based on the initial tests the expression from Kofoed (2002) has been updated to include geometries with fronts mounted on the individual reservoirs. Using this updated expression the crest levels have been optimized to fit the prevailing wave conditions at the prototype location. Further model tests have been performed leading to further optimization of the geometry of the structure.

After taking into account the effect of wave directions and structure orientation it has been found that for the optimized structure the overall average hydraulic efficiency at the prototype location for a structure facing due west (270°) is 41.4 % for near shore wave conditions corresponding to offshore wave conditions 1-7. This corresponds to an overall average hydraulic power production of 7.5 kW/m.

However, the wave directions and structure heading has been taken into account using a correction factor derived from model tests with 2-D waves and shore protection structures (breakwaters and dikes), and not a multi level structure with a relatively small width. Thus, there is a considerable uncertainty in using it for the current purpose and 3-D tests with more detailed modeling of foreshore and structure is needed in order to include refraction/diffraction effects around the structure.

Further testing of a 3-D model of the structure in oblique and 3-D wave conditions are scheduled for this autumn. These tests will also include measurements of local and global forces on the structure to enable a reliable structural design.

NOMENCLATURE

A, B, C	Regression coefficients [-].
dq/dz	Derivative of the overtopping rate with respect to the vertical distance z [m^3/s/m/m].
g	Gravitational acceleration, 9.82 m/s^2
H_s	Significant wave height [m].
P_n	Hydraulic power pr. width of n'th reservoir [kW/m], calculated as qR_cg.
P_{total}	Sum of P_n over all reservoirs [kW/m].
P_{wave}	Available wave power [kW/m], calculated as $P_{wave} = \frac{\rho g^2}{64\pi} T_e H_s^2$
q	Overtopping rate pr. width [m^3/s/m].
Q	Non-dimensional overtopping rate [-].
Q'	Dimensionless derivative of the overtopping rate with respect to z [-].
q_n	Overtopping rate pr. width of n'th reservoir [m^3/s/m].
q_{total}	Sum of q_n over all reservoirs [m^3/s/m].
R	Relative crest freeboard [-].
R_c	Crest freeboard [m]
$R_{c,n}$	Crest level of n'th reservoir [m].
T_e	Wave energy period [s], here estimated as T_p/1.15.
T_p	Wave peak period [s].
z	Vertical distance [m].
α	Angle of front slope [°].
β	Wave direction, 0° head-on [°].
γ_β	Factor accounting for oblique wave attack [-].
λ_s	Factor accounting for low R [-].
λ_β	Correction factor derived from γ_β for multiplication onto q_n [-].

REFERENCES

Kofoed J. P. (2002): *Wave Overtopping of Marine Structures – Utilization of Wave Energy*. Ph. D. Thesis, defended January 17, 2003 at Aalborg University. Hydraulics & Coastal Engineering Laboratory, Department of Civil Engineering, Aalborg University, December, 2002.

Kofoed, J. P.: *Model testing of the wave energy converter Seawave Slot-Cone Generator*. Hydraulics and Coastal Engineering No. 18, ISSN: 1603-9874, Dep. of Civil Eng., Aalborg University, April 2005.

Kofoed, J. P. and Guinot, F.: *Study of Wave Conditions at Kvitsøy Prototype Location of Seawave Slot-Cone Generator*. Hydraulics and Coastal Engineering No. 25, ISSN: 1603-9874, Dep. of Civil Eng., Aalborg University, June 2005.

Kofoed, J. P.: *Experimental Hydraulic Optimization of the Wave Energy Converter Seawave Slot-Cone Generator*. Hydraulics and Coastal Engineering No. 26, ISSN: 1603-9874, Dep. of Civil Eng., Aalborg University, June 2005.

Torsethaugen, K. (1990): *Bølgedata for vurdering av bølgekraft*, SINTEF NHL-report No. STF60-A90120, 1990-12-20, ISBN Nr. 82-595-6287-1.

Van der Meer, J. W. and Janssen, J. P. F. M. (1995): *Wave run-up and wave overtopping at dikes.* Technical report, Task Committee Reports, ASCE.